

New Results on Pb-Au Collisions at 40 AGeV from the CERES/NA45 Experiment

K. Filimonov^{1*}, D. Adamová[†], G. Agakichiev^{**}, H. Appelshäuser^{*}, V. Belaga[‡],
 P. Braun-Munzinger^{**}, A. Cherlin[§], S. Damjanović^{*}, T. Dietel^{*}, A. Drees[¶],
 S. I. Esumi^{*}, K. Fomenko[‡], Z. Fraenkel[§], C. Garabatos^{**}, P. Glässel^{*}, G. Hering^{**},
 V. Kushpil[†], B. Lenkeit^{||}, A. Maas^{**}, A. Marín^{**}, J. Milošević^{*}, A. Milov[§],
 D. Miśkowiec^{**}, Y. Panebrattsev[‡], O. Petchenova[‡], V. Petraček^{*}, A. Pfeiffer^{||},
 J. Rak^{**}, I. Ravinovich[§], P. Rehak^{††}, H. Sako^{**}, W. Schmitz^{*}, J. Schukraft^{||},
 S. Sedykh^{**}, W. Seipp^{*}, S. Shimansky[‡], J. Slívová^{*}, H. J. Specht^{*}, J. Stachel^{*},
 M. Šumbera[†], H. Tilsner^{*}, I. Tserruya[§], J. P. Wessels^{*}, T. Wienold^{*}, B. Windelband^{*},
 J. P. Wurm^{††}, W. Xie[§], S. Yurevich^{*} and V. Yurevich[‡]

**Universität Heidelberg, Germany*

†NPI/ASCR, Řež, Czech Republic

***GSI, Darmstadt, Germany*

‡JINR, Dubna, Russia

§Weizmann Institute, Rehovot, Israel

¶Department for Physics and Astronomy, SUNY Stony Brook, USA

||CERN, Geneva, Switzerland

††Brookhaven National Laboratory, Upton, USA

‡‡Max-Planck-Institut für Kernphysik, Heidelberg, Germany

INTRODUCTION

Low-mass dilepton spectra are expected to provide information on the early stage of the relativistic heavy-ion collisions which may experience an onset of deconfinement and/or chiral symmetry restoration. The CERES/NA45 measurements of e^+e^- -pair production in 158 AGeV Pb-Au collisions revealed a significant excess of the dielectron yield over known hadronic sources in the invariant mass region $0.25 < m_{ee} < 0.7$ GeV/c² [1]. The enhancement is mostly observed for pairs with low transverse momentum $p_{t}^{ee} < 0.5$ GeV/c and increases stronger than linearly with the event multiplicity. These experimental data have stimulated extensive theoretical discussions on the mechanisms of low-mass dilepton production and emission from hot and dense hadronic medium (for a review see [2]). The thermal radiation from the interaction phase of the hadronic fireball via annihilation processes, predominantly $\pi^+\pi^- \rightarrow \rho \rightarrow e^+e^-$, may account for a large fraction of the observed enhancement. The spectral shape in the mass region of the excess, however, cannot be described and requires introducing in-medium effects on the ρ spectral function. Two scenarios that take into account in-medium modifications of the vector meson properties have been particularly successful in reproducing the CERES results. One assumes a reduction of the ρ -meson mass in the hot and dense medium as a precursor of chiral symmetry restoration [3], following Brown-Rho scaling [4]. Another approach uses a ρ -meson spectral function which takes into account modifications of meson properties due to interactions with the surrounding hadrons [5]. Dilepton production rates and shapes of the invariant mass spectra in these two calculations are very similar pointing to a shift of the hadron-parton duality threshold towards lower masses [6]. The measurement of dilepton spectra at lower beam

¹ Present address: LBNL, Berkeley, USA

energy of 40 AGeV allows to study the effect of varying the baryon density and provides additional constraints for the model calculations. It is also the first measurement after upgrading the CERES spectrometer with a Time Projection Chamber to provide a better resolution in the mass region of the narrow resonances ω and ϕ .

EXPERIMENTAL SETUP

The CERES spectrometer (Figure 1) is optimized to measure electron pairs at midrapidity ($2.1 < \eta < 2.6$) with full azimuthal coverage. Two silicon drift chambers (SIDC1,2) located 10 cm and 13.8 cm behind a segmented Au target provide a precise angular measurement of charged particles and vertex reconstruction. The electrons are identified by the two Ring Imaging Cherenkov detectors (RICH1,2) operated at a $\gamma_{\text{th}} = 32$, which rejects 95% of all charged hadrons. The momentum of all charged particles is measured by the radial drift Time Projection Chamber (TPC) [7]. The TPC has an active length of 2 m and an outer diameter of 2.6 m and provides the measurement of 20 space points in a magnetic field with a maximal radial component of 0.5 T.

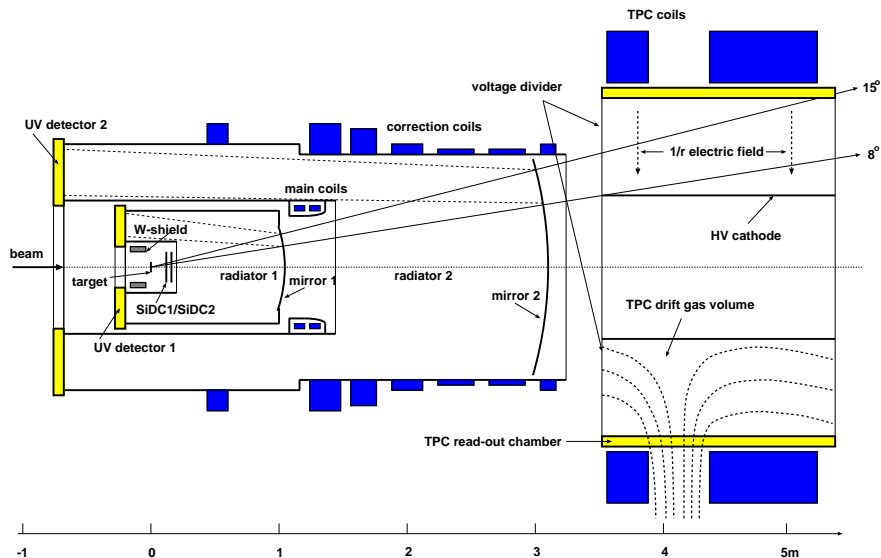


FIGURE 1. The upgraded CERES spectrometer at the CERN-SPS

The data taking period in the fall of 1999 was the first run of CERES after the TPC upgrade. Due to problems with the new readout the data set is limited in statistics and TPC efficiency. In total we recorded 8.7M Pb-Au events at 40 AGeV with centrality $\sigma/\sigma_{\text{geo}} \approx 30\%$.

ELECTRON-POSITRON PAIR ANALYSIS

The dominant sources of e^+e^- -pairs are photon conversions and π^0 -Dalitz decays which are characterized by the small pair opening angle and invariant masses below $200 \text{ MeV}/c^2$. The large number of such pairs ($N_{e^+e^-}(m < 200 \text{ MeV}/c^2)/N_{e^+e^-}(m > 200 \text{ MeV}/c^2) \sim 10^4$) combined with limited track reconstruction efficiency and acceptance results in a combinatorial background for events with two partially reconstructed low-mass pairs. This combinatorial background can be significantly reduced by pairing only tracks with transverse momentum $p_t > 200 \text{ MeV}/c$. To remove the hadronic contamination in accidental matching between RICH and TPC we use dE/dx information from the TPC. Conversions and Dalitz pairs with opening angle less than 10 mrad which are not recognized as two individual rings in the RICH detectors are rejected by a double energy loss cut in the two SIDC detectors. To account for a limited TPC efficiency in the 1999 data set, we also remove tracks which have a SIDC-RICH electron candidate within 70 mrad. Finally, identified Dalitz pairs ($m_{ee} < 200 \text{ MeV}/c^2$) are excluded from further combinatorics. The signal is extracted by subtracting like-sign pairs from unlike-sign pairs. The total number of open pairs ($m_{ee} > 200 \text{ MeV}/c^2$) is 180 ± 48 (stat.) with a signal-to-background ratio of 1/6.

The measured e^+e^- invariant mass spectrum is compared to the hadronic cocktail in Figure 2 (left). The data were

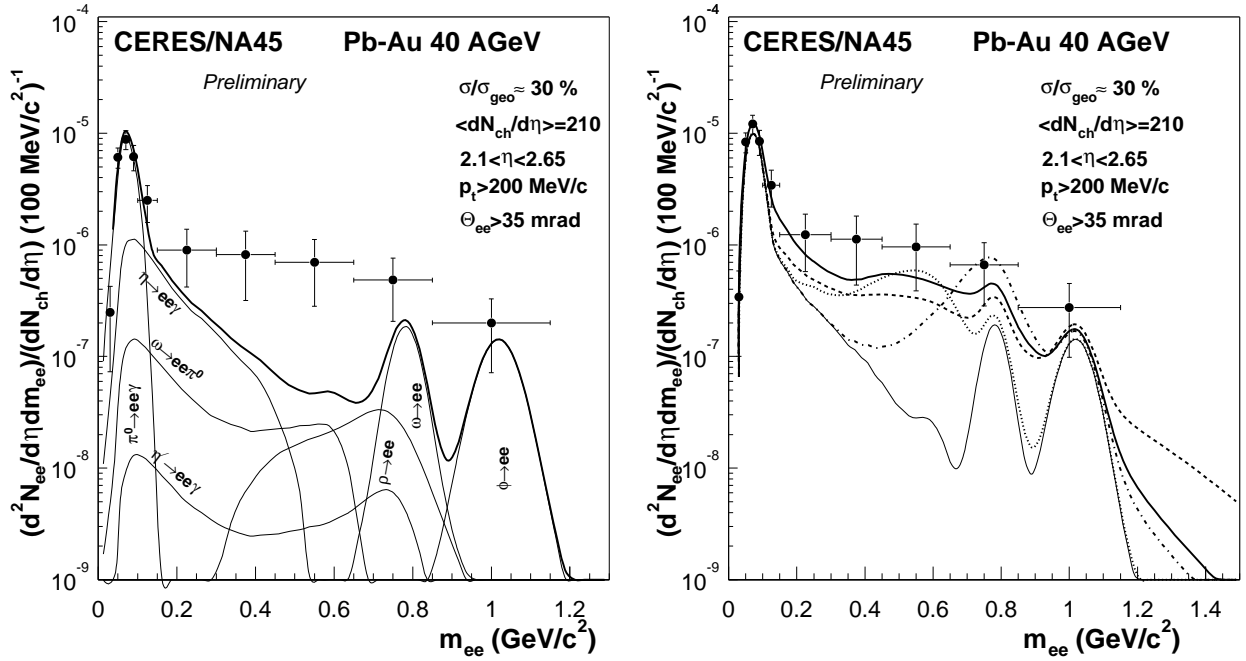


FIGURE 2. Inclusive e^+e^- invariant mass spectrum at 40 AGeV in comparison to expectations from known hadronic sources in heavy ion collisions ('hadronic cocktail') (left) and in comparison to model calculations (right) assuming the vacuum ρ spectral function (dash-dotted), a dropping ρ mass (dotted) and including medium modifications of the ρ spectral function (thick solid line). Also shown is the hadronic cocktail without ρ (thin solid line). The dashed line refers to a lowest order pQCD rate calculation. All calculations are from [8].

normalized to the hadronic cocktail in the π^0 -Dalitz region. Similar to the observations at 158 AGeV, the measured e^+e^- yield exhibits an enhancement by a factor of 5.0 ± 1.5 (stat.) in the mass range $m_{ee} > 200$ MeV/ c^2 compared to the expectations from known hadronic sources in heavy-ion collisions. The excess is most pronounced for pairs with small transverse momentum. The results are also compared to different theoretical calculations in Figure 2 (right). The measurements clearly disfavor a purely hadronic scenario assuming the vacuum ρ spectral function.

HADRON SPECTRA AND YIELDS

The addition of the TPC allowed for a systematic investigation of hadronic observables around midrapidity. The matching requirement to the SIDC system leads to a very efficient suppression of non-vertex tracks. On the other hand, using SIDC detectors as a veto improves the signal-to-background ratio for the reconstruction of Λ and K_S^0 . The measured transverse mass distributions of negatively charged hadrons h^- and proton-like positive net charges '(+) - (-)' are shown in Figure 3 in different bins of rapidity for events with centrality $\sigma/\sigma_{geo} < 15\%$. The solid lines represent the best fits to the spectra using an exponential $1/m_t dN/dm_t \propto \exp(-m_t/T)$. The rapidity averaged slopes ($T_{h^-} = 176 \pm 5$ MeV and $T_{(+)-(-)} = 278 \pm 12$ MeV) are similar to those observed at top AGS and SPS energies, with only a weak dependence on centrality. The large difference between h^- and (+) - (-) slopes indicates the presence of strong radial flow also at 40 AGeV. The midrapidity yield of h^- as function of N_{part} (Figure 3, right) rises significantly stronger than linear, while a rise with $N_{part}^{1.07 \pm 0.04}$ at top SPS energy has been reported recently [9]. This points to a change in the particle production mechanism going from 40 AGeV to 158 AGeV. In fact, a strongly non-linear behaviour has also been observed at the AGS [10]. The non-linear rise of the midrapidity (+) - (-)-yield with N_{part} is possibly caused by an increasing amount of stopping, in agreement with the UrQMD prediction.

We have also identified Λ hyperons by invariant mass reconstruction [11]. The measurements cover the rapidity range from $y = 2.0$ to 2.4 and transverse momenta from $p_t = 0.9$ GeV/ c to 2.5 GeV/ c . Λ transverse momentum spectra have been fitted by an exponential in the three centrality intervals (Figure 4, left). The extracted inverse slope parameters are shown in Figure 4 (right). The Λ slopes measured at 40 AGeV are within errors consistent with those

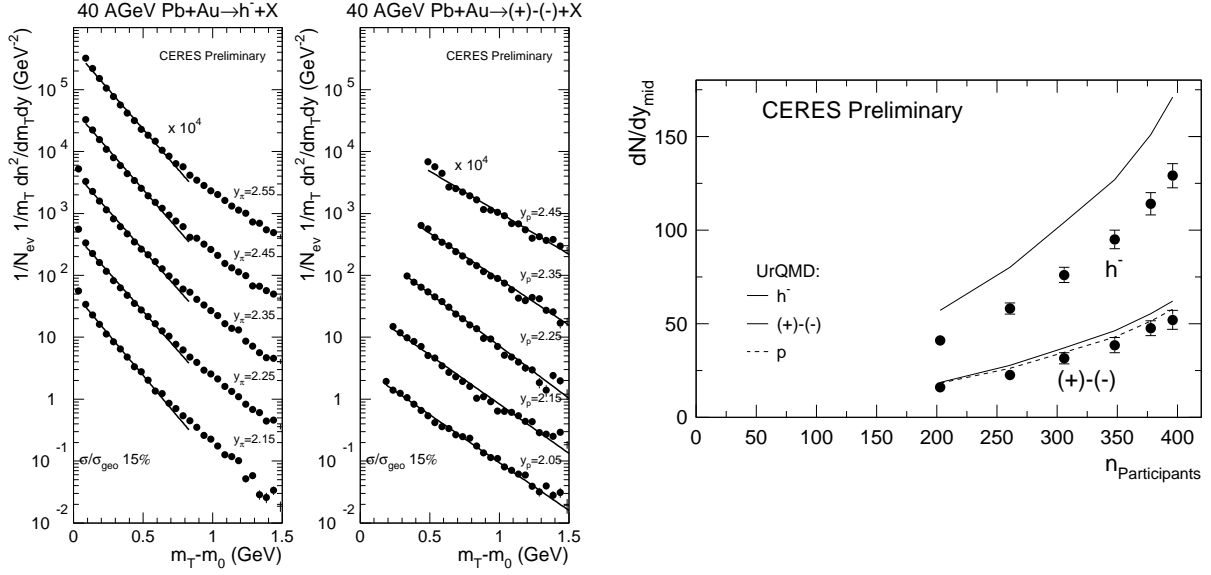


FIGURE 3. Left panel: Measured h^- (left) and proton-like positive net charges (right) transverse mass spectra for events with centrality $\sigma/\sigma_{geo} < 15\%$. Beginning with the lowest rapidity bin the spectra have been multiplied by a successive factor of 10. The lines are the exponential fits to the data. Right panel: Midrapidity yields of h^- and $(+)-(-)$ as a function of number of participants. Also shown are results from UrQMD.

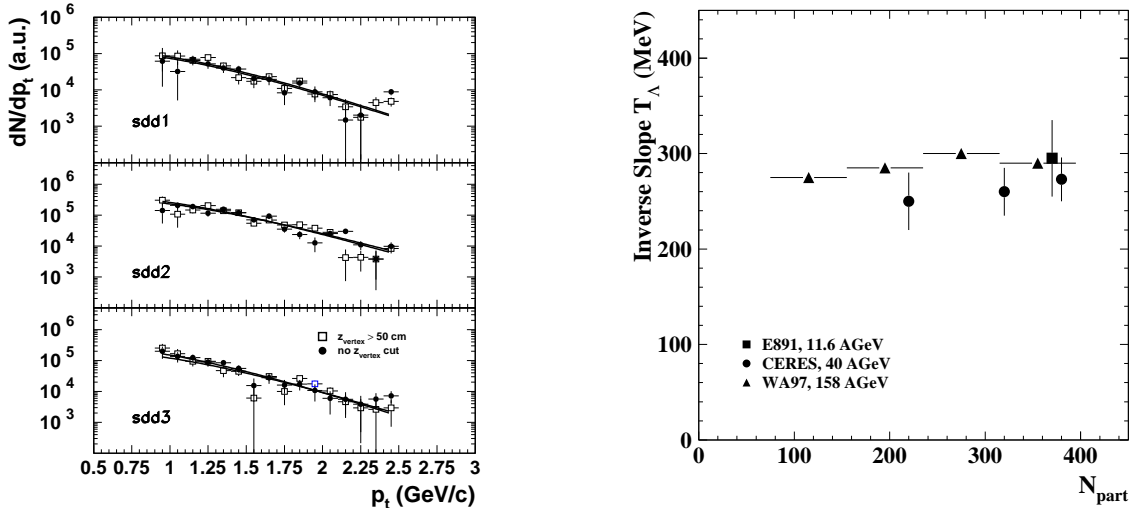


FIGURE 4. Left: Measured Λ transverse momentum spectra for the three centrality intervals. The solid lines are the exponential fits to the data. Right: Λ inverse slope parameters as a function of number of participants.

at the top SPS energy [12] and AGS [13]. They are also very similar to the parameters extracted from spectra of proton-like positive net charges. By integrating the spectra where the data are available and using the results from the exponential fits to extrapolate to infinity and to $p_t=0$ we obtained the yield of Λ -hyperons in the measured rapidity interval: $dN/dy_\Lambda = 11 \pm 2$ for centrality $\sigma/\sigma_{geo} < 5\%$. We have also measured the ratios of $\Lambda/p = 0.22 \pm 0.05$ and $\bar{\Lambda}/\Lambda = 0.024 \pm 0.010$ for the same centrality.

DIRECTED AND ELLIPTIC FLOW

Anisotropies in the azimuthal distribution of particles, also called anisotropic (directed, elliptic, etc.) transverse flow, have proven to be sensitive to the initial pressure in the collision region and the degree of thermalization during the expansion stage. Our flow analysis is based on the azimuthal hit distributions in the SIDC1,2. The two coefficients v_1 and v_2 , respectively quantifying the strength of directed and elliptic flow, are obtained from a Fourier decomposition of the azimuthal charged particle distribution with respect to the orientation of the reaction plane [14]. The v_1 and v_2 values have been corrected for the finite reaction plane resolution, determined by the subevent method. The pseudorapidity dependence of directed and elliptic flow measured at 40 AGeV is presented in Figure 5 (left) for three

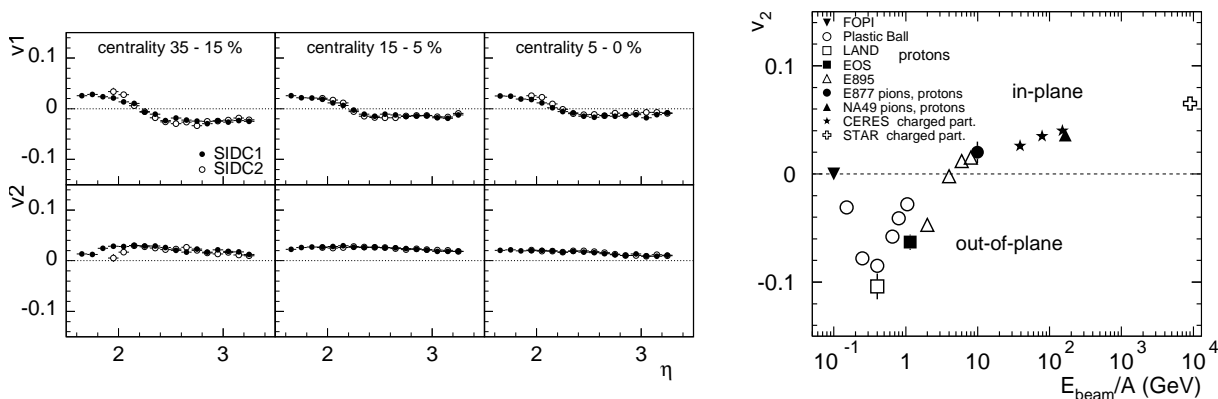


FIGURE 5. Left: Pseudorapidity dependence of directed (v_1) and elliptic (v_2) flow at 40 AGeV for three centrality intervals. Right: v_2 as a function of the beam kinetic energy for semi-central collisions of Pb or Au nuclei.

different centralities. While v_1 exhibits the characteristic zero-crossing at midrapidity, v_2 is positive and independent of pseudorapidity. We have also performed the measurements of elliptic flow at 80 and 158 AGeV. The v_2 -values increase with beam energy (Figure 5, right) and fit smoothly into the measured systematics.

OUTLOOK

In the fall of 2000 we took a sample of 33M central Pb-Au events at 158 AGeV with a very good overall performance of the spectrometer. The analysis of the 2000 data will provide a long-awaited dilepton invariant mass spectrum with the mass resolution $\Delta m/m < 2\%$ in the region of ω and ϕ resonances. The systematic hadron analysis of data taken at 40, 80 and 158 AGeV is in progress, including results on HBT-interferometry and mean transverse momentum fluctuations [15].

REFERENCES

1. Agakichiev, G., et al. (CERES Collaboration), *Nucl. Phys. A*, **661**, 23 (1999).
2. Rapp, R., and Wambach, J., *Adv. Nucl. Phys.*, **25**, 1 (2000).
3. Li, G., Ko, C., and Brown, G., *Phys. Rev. Lett.*, **75**, 4007 (1995).
4. Brown, G., and Rho, M., *Phys. Rev. Lett.*, **66**, 2720 (1991).
5. Rapp, R., Chanfray, G., and Wambach, J., *Nucl. Phys. A*, **617**, 472 (1997).
6. Rapp, R., *Nucl. Phys. A*, **661**, 33 (1999).
7. Agakichiev, G., et al. (CERES Collaboration), *Nucl. Phys. A*, **661**, 673 (1999).
8. Rapp, R. (2001), private communication.
9. Aggarwal, M., et al. (WA98 Collaboration), *Eur. Phys. J. C*, **18**, 651 (2001).
10. Ahle, L., et al. (E802 Collaboration), *Phys. Rev. C*, **59**, 2173 (1999).
11. Schmitz, W., *A Production in Pb-Au Collisions at 40 AGeV*, Ph.D. thesis, Heidelberg University (2001).
12. Sandor, L., et al. (WA97 Collaboration), *Nucl. Phys. A*, **661**, 481 (1999).
13. Ahmad, S., et al. (E891 Collaboration), *Phys. Lett. B*, **382**, 35 (1996).
14. Voloshin, S., and Zhang, Y., *Z. Phys. C*, **70**, 665 (1996).
15. Adamová, D., et al. (CERES Collaboration), *Nucl. Phys. A* (2001), proceedings of Quark Matter 2001, in press.